Reliable and Efficient Simulation of Nets for Active Space Debris Removal Purposes

W. Gołębiowski, R. Michalczyk
SKA Polska Sp. z o.o., Poland
e-mail: w.golebiowski@ska-polska.pl

M. Dyrek, Z. Derda
OptiNav Sp. z o.o., Poland
e-mail: m.dyrek@optinav.pl

U. Battista
Stam S.r.l., Italy
e-mail: u.battista@stamtech.com

K. Wormnes
Automation and Robotics Section, ESA
e-mail: kjetil.wormnes@esa.int

Abstract

One of considered methods for capturing large orbital debris is elastic deployable net. For analysis of capturing scenarios, ADR mission planning and net design purposes a validated and efficient net simulator is required. A robust mathematical model for thin elastic rods dynamics and its implementation for parametric net simulation are presented in this paper. Used model reproduces most important properties of thin elastic structures (which are used for nets manufacturing): stretching, bending and torsion (including damping in these directions). Comparison to FEM results and initial experimental validation are discussed. Full validation approach is also described. Validation experiments will be performed with down scaled net model in microgravity environment – during parabolic flight.

1 Introduction

In almost 50 years of space activities more than 4800 launches have placed some 5000 satellites into orbit, of which only a minor fraction of about 1000 are still operational today. Besides this large amount of intact space hardware, with a total mass of about 6000 tones, several additional objects are known to orbit the Earth. They are regularly tracked by the US Space Surveillance Network and, today, more than 16 000 of them are maintained in their public catalogue, Only 6% of the catalogued orbit population are operational spacecraft, while 28% can be attributed to decommissioned satellites, spent upper stages, and mission related objects. The remainder of about 66% is originating from more than 200 on-orbit fragmentations which have been recorded since 1961. These are assumed to mainly have generated a population of objects larger than 1 cm on the order of 700 000. So far, there are four recorded examples of collisions (with the latest and most prominent one between the active Iridium-33 satellite and the decommissioned Cosmos-2251 satellite). Today there is a great concern and consensus that collisions could become the main future source for new debris objects, leading the space debris environment into a chain reaction, rendering some orbital regions with an unacceptably risk for operations.

Studies at NASA and ESA [1, 2] showed that the environment can be stabilized when on the order of 10 objects are removed from LEO per year with a removal sequence oriented towards the target mass. Active removal can be more efficient in terms of the number of collisions prevented / object removed, when objects removed have high mass, high collision probabilities and high altitudes.

ESA, with its Clean Space initiative, devotes increasing attention to the environmental impact of its activities, including its own operations and operations performed by European industry in the frame of ESA programs, through the implementation of specific technology roadmaps. The Clean Space initiative, organizes the implementation around four distinct branches, 1) Eco-design, 2) Green technologies, 3) Space debris mitigation and 4) Space debris remediation. Branch 4 aims to start the development and demonstration of the key technologies required for the capture and controlled atmospheric re-entry of an uncooperative target orbiting in the LEO protected region. Currently, a number of technology developments are under-way with many more planned [4].

Over many years, ESA, together with industrial partners, have found throw-nets to be a particularly promising technology for capturing objects in space in cases where robot grasping will be difficult [3, 5] (targets may have unpredictable spins and no suitable grasping points), such as is the case in general for space debris. The technology development detailed in this paper (funded by ESA's Technology Research Program (TRP) under branch 4 of the Clean Space initiative) aims at developing a validated simulator for the capture of a large space debris with a throw-net, and to demonstrate the capture on a parabolic flight.

As described simulator is intended to use for mission planning, individual design of the net or sensitivity analysis, the underlying model should be a reasonable compromise between performance and physical accuracy. Thus the validation aspect is particularly important.

2 Model Description

Net can be treated as a system of threads linked together with knots. Single thread can be modeled as 1-dimensional element using special rod theory. We assume that rod is a structural member, long and slender, and is capable of carrying load along its axis via elongation and bending loads applied transverse to its long axis. This problem can be generally approached from standpoint of the methods of strength of materials, which simplify 3-dimensional theory of elasticity and reduce it to 1-dimensional. Strains and stresses are generalized and seen as internal forces called bending torques and tension. The deformation is usually studied by defining the position and the orientation of its start- and end points, which results in a boundary value problem.

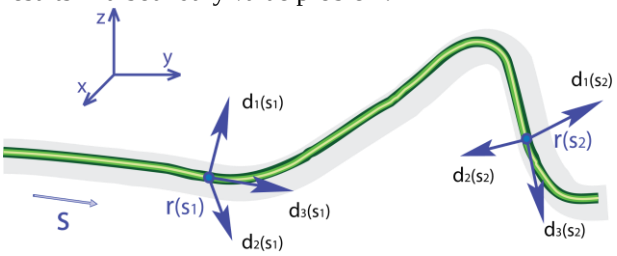

*Fig. 1 A simple Cosserat model, **s** -the curvilinear coordinate along the centerline of the undeformed rod.*

Since nets deformations are large, the general dynamical theory of rods that can undergo large displacements and geometrical nonlinearities is needed. Mathematical models constructed on the basis of classical beam theories (particularly Bernoulli-Euler or Timoshenko) are not sufficient in this case. Instead, special case of geometrically exact theory with intrinsic directions at each point, called the Cosserat theory of rod, is used. A comprehensive introduction to this is provided in the book of Antman [6]. Further studies on the dynamic formulation of elastic rods have been presented in [7]. Simulation of nets demand the capability to numerically capture geometric nonlinearities in a predictive and efficient way. These nonlinear kinematic effects arise from the large displacements and rotations of the slender structure, even if its material properties remain linear throughout the process. Presented approach is very popular nowadays in the field of computer graphics simulation and was introduced by Pai [8]. Recently, a new modeling strategy to discretize the rod and to derive the ordinary differential equations of motion has been proposed by Spillmann [9].

Detailed formulation of kinematics of the slender elastic rod may be found in literature, here we only briefly present the concept. At large scales, the rod can be regarded as an adapted material curve: its centerline. Cosserat deformation models consider an oriented centerline, i.e. in each point of the continuous curve, we can think of an orthonormal basis that conforms to the material frame. It means that additional degrees of freedom are necessary to express the orientation of the centerline and reproduce both bending and twisting deformation. It is therefore convenient to introduce an orthonormal basis $\mathbf{d_i(s, t)}$ **(i=1,2,3)** of a cross-section at every point, termed the moving basis, such that $\mathbf{d_3}$ is normal to the rotated cross-section, and $\mathbf{d_1}$ and $\mathbf{d_2}$ lie in the plane of the rotated cross-section (Fig. 1). This way in the sense of Cosserat theory, the motion of rods in three-dimensional space can be demonstrated by its neutral axis $\mathbf{r(s, t)}$ (curve) and 3 orthogonal unit vectors $\mathbf{d_i(s, t)}$ (directors).

To establish the stress-strain relation, a quantity has been introduced that measures the rate of change in the position and orientation at every point of rod centerline. As usually for slender structures, shearing is neglected, only the stretch along the centerline is measured. The change of orientation in the reference frame is measured by differential geometry quantity called Darboux vector.

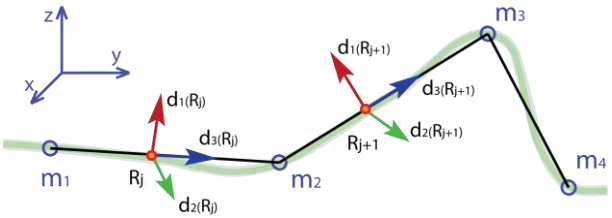

Fig. 2 Discretized Cosserat rod model

There is a number of choices for the parameterization of rotation matrix. Here, the change in orientation is described by means of quaternions, a number system that extends the complex number representation of geometry in a plane to the three-dimensional space and produces non-singular representation of rotation. In consequence we have three linear DoFs and four quaternion coordinates that constitute the seven degrees of freedom of elastic rod. After taking into account constraint equations, only three of them are, in fact, geometrically independent. Their values are determined by the three-dimensional equilibrium equations.

The equations for equilibrium can be derived under the assumption that this energy is stationary under small deformations. The stretch energy is defined to be a quadratic form in the stretch along centerline while

bending and twisting energy is a quadratic form in the strain rate vector measuring the change of orientation. The internal friction, that reduces oscillations, is also considered. Since strains at material level are usually small the linear constitutive laws are considered.

The principle of virtual work is used to derive the ordinary differential equations of motion, based on the Lagrangian (1) constructed by the Cosserat kinetic (E), strain (V), dissipation (D) and constraints (C) energy expressions.

$$\frac{d}{dt}\frac{\partial E}{\partial \dot{q}_i} - \frac{\partial E}{\partial q_i} + \frac{\partial V}{\partial q_i} + \frac{\partial D}{\partial \dot{q}_i} + \frac{\partial C}{\partial q_i} = F \qquad (1)$$

There are severe limitations of theoretical closed form solutions, mainly idealizations that are assumed to facilitate the mathematical solution. However, problems can be solved using advantages of approximations and numerical methods. Most popular and powerful method of discretization of rod differential equations, Finite Element Method (FEM), has been used for reduction of continuum system to a system with finite number of degrees of freedom. Having continuous deformation energies (functions of the strains), we discretized the rod and derive energy for each element. The position of the rod is represented by discretizing its centerline into elements separated by control points. The orientations of the elements are represented by material frames. To compute the element energies, the unknown displacement field has to be approximated, using constant shape functions.

The discrete Lagrangian equation of motion that characterizes the dynamic equilibrium is obtained by substituting discrete energies into (1). This results in a system of the form (2).

$$M\ddot{q} + C\dot{q} + Kq = F \qquad (2)$$

Because of simplifications introduced to the system (geometric constraints expressed by energy function) equation (2) can be solved directly without inverting mass matrix. The rod can be considered as a chain of control points and a chain of quaternions conforming to the material frames. These chains are loosely coupled by penalty forces that accelerate them towards a valid configuration. The approach is presented in [9]. The explicit simulation of the quaternions enables a convenient computation of the material direction, which allows a direct solve of the equations of motion, resulting in a comparably small implementation effort.

3 Early Results

Numerical experiments were performed to validate the physical behavior of the proposed model, verify numerical stability, and test the performance. The numerical code is an implementation of the mechanical model briefly presented in previous section. Presented results include: (1) comparison between experimental and numerical records of pure bending test, (2) implementation of the physical pendulum test, as it's a common test in the literature, (3) simulation of net flight, impact and capture sequence.

There are various standard approaches for investigating behavior of threads. The common method is based on deformation of specimen under its own weight [11]. This approach is called cantilever test method and calculates bending behavior of filament by determining its bending resistance. To verify accuracy and precision of proposed model we first consider a simple experiment as described in section 4.2. Pure elastic bending of an 8 cm polypropylene yarn with one edge fixed (cantilever beam) was recorded. Specimen was loaded with its own uniformly distributed weight.

Numerical model consists of 11 equally length segments. All degrees of freedom at left end were fixed. The beam was initially in horizontal position and the gravitational force was applied. Resultant curve after achieving equilibrium is shown in Fig. 3. Comparison showed good agreement between predicted and measured bending characteristics. Also for damped oscillations around final position.

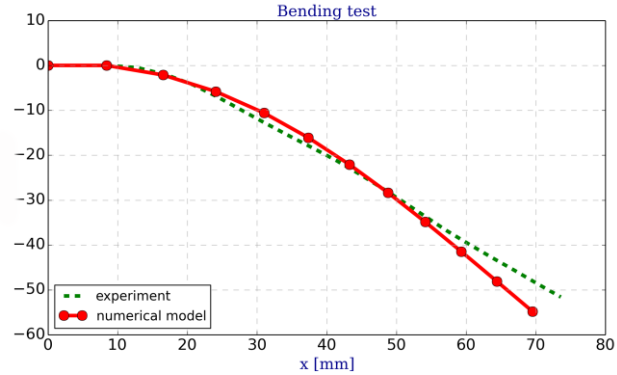

Fig. 3 Pure bending test. Experimental result and numerical model comparison.

Next the results of the numerical simulations using the implemented model were compared to simple elastic pendulum. This case study is well described in the literature and widely used when it comes to test mechanical models of cord or twine (see [10]). However researchers mostly refer to numerical experiments and we are not aware of any real measurements for this type of test. Evolution of a system in time is usually tested using recognized models, classical beam theory for example. That is why commercial finite element code (ABAQUS)

have been used to create a reference 1D model, mainly because it already combines standard routines in dealing with standard finite elements, time integration and contact algorithms including comprehensive tools for pre- and post-processing.

The scenario was the same for Cosserat and FEM model. Initially at t = 0, the rod was completely straight, not pre-deformed, aligned along the global x-axis and discretized equidistantly. Thus in case of Cosserat rod the directors for material frame were $d_1(0) = y$, $d_2(0) = z$, $d_3(0) = x$ at t = 0. The gravitational acceleration g = $9.81 ms^{-2}$ was acting along the negative y-direction. Dynamically swinging pendulum yarn of 30 cm length and circular cross section was subdivided into N = 11 segments. Material properties were chosen based on material characterization as previously.

For both tests explicit method was used for time integration. We focused on short initial phase of the yarn fall (from t=0 to t=0.5s) which included the most interesting process – the evolution of peak in the velocity time dependence of the tip.

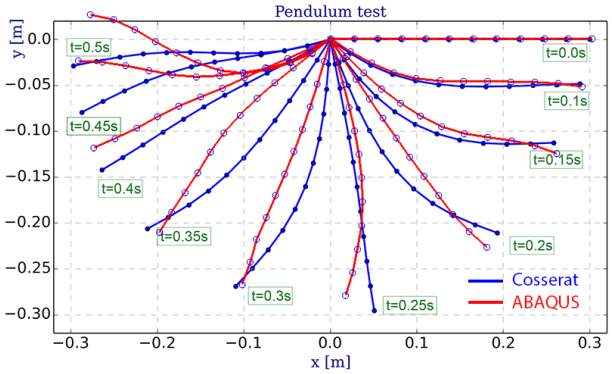

Fig. 4 Snapshot of the dynamic pendulum test (Cosserat vs FEM model).

Some snapshots of the scenario are depicted in Fig. 4. It also shows moderate agreement between our model and corresponding Abaqus 1D solution, computed with beam elements. Differences in the solutions occur for the reason that not only the curvature, but as well the continuous Cosserat strain differs from the one that Abaqus uses. It should be denoted that Cosserat rod model computes numerical results at lower computational cost.

The most interesting case and main reason of all investigations is of course net flight and capture sequence. In the dynamical analysis, the capture process is highly nonlinear, because the deformation (even if the material is pure elastic) may be extremely large.

We considered simple scenario when simplified planar net catches a spherical body. The detailed net system characteristics: dimension 1x1 m, composed of the same polypropylene tethers as in previous examples. Each link connecting knots has length of 20 cm and is discretized in N=5 elements. The whole net is composed of 276 nodes and 300 segments. Four bullets (mass of 0.5 kg each) are attached to knots at corners. The net is falling due to gravitational force on a rigid sphere. Simplified contact algorithm is used.

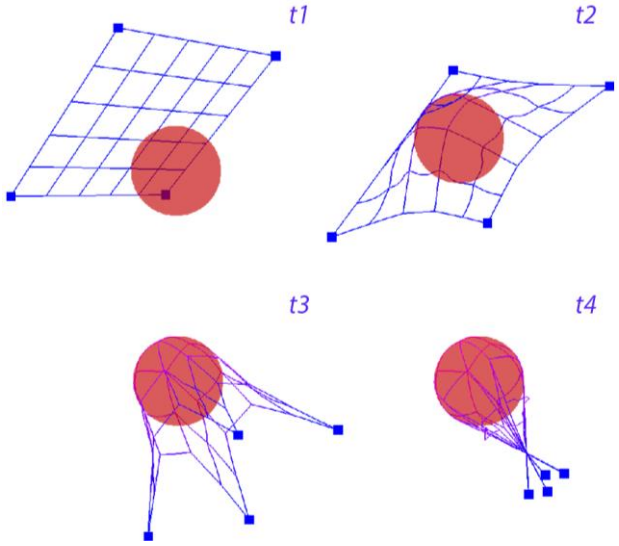

Fig. 5 Net capture sequence – FEM Abaqus solution.

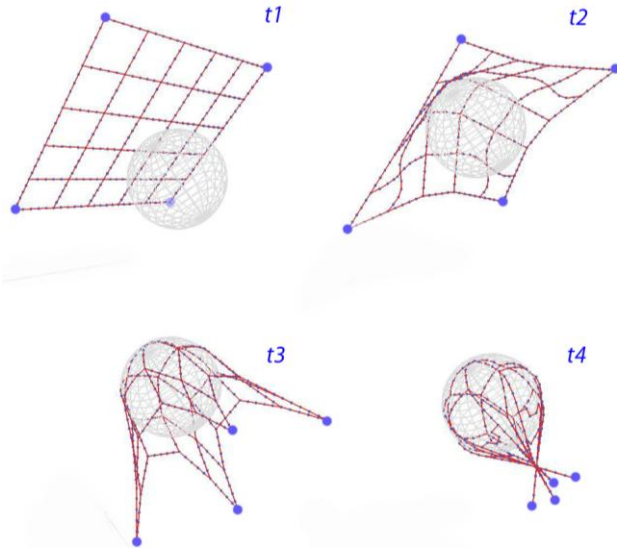

Fig. 6 Net capture sequence – Cosserat rod solution.

Similar analysis was prepared using Abaqus software. Dimensions, discretization and initial conditions were the same. The only difference was more sophisticated contact algorithm. In both cases explicit time integration was used. Few snapshots of the scenario for both models are depicted in Fig. 5 and Fig. 6. Times when results were recorded: t1=0, t2=0.1, t3=0.2, t4=0.3 s.

These first tests were focused on checking if Cosserat rod model, which implementation is based on [9], is useful to simulate net dynamics and capture process. Comparison of net behavior obtained indicates that both FEM and Cosserat rod model can reproduce similar results. These experiments however can't be treated as validation of the model because it has not been proven that FEM beam theory is suitable to reproduce real net behavior. That is why there is need to validate this kind of simulations with physical experiments.

4 Validation

4.1 Methodology

Model validation methodology is based on preparation of experiments for representative cases of debris capturing process with a net. Experiments will cover all the phases of debris capturing: net launch, free flight and target wrapping.

Due to the nature of modeled phenomena experiment has to be performed in microgravity conditions, during parabolic flight. Geometrical and time constraints of parabolic flight require to downscale the experiment: the net and model of the target will be 25 times smaller than for real application of space debris capturing. Other quantities like masses, velocities and net material properties has to be scaled as well according to similitude principles. As a result four experimental cases are being prepared:

1. Net A (1x1 m, 10 cm mesh size, 1 mm Nylon thread, knotted assembly), velocity: 0.5 m/s, distance: 2 m
2. Net A, velocity: 0.8 m/s, distance: 2 m
3. Net B (1x1 m, 6 cm mesh size, 1 mm Nylon thread, knotless assembly), velocity: 0.5 m/s, distance: 2 m
4. Net B, velocity: 0.8 m/s, distance: 2 m

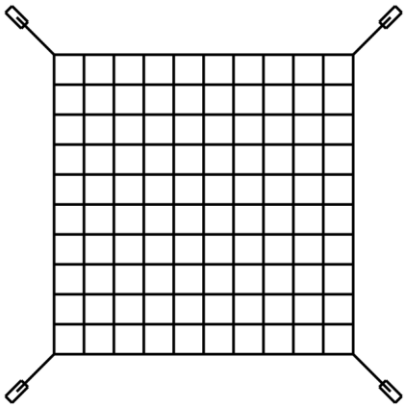

Fig. 7 Structure of the experimental net (Net A)

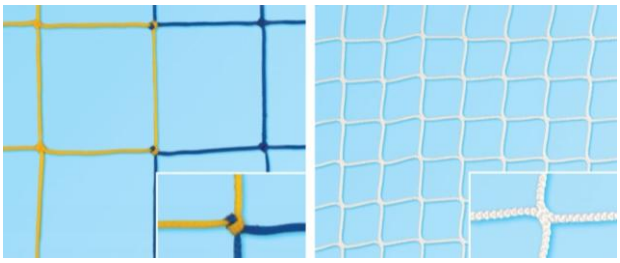

Fig. 8 Knotted (left) and knotless (right) net assembly technology

For the parabolic flight campaign 20 parabolas are planned, each with microgravity period of about 18 s. Each of the experimental cases will be repeated 5 times for statistical significance.

For performing the experiments special testing rig is being built, which comprises of:

- Quick reloadable net ejector with controllable speed and net corner masses ejection angles (to control a speed of net development during flight)
- Simplified model of satellite to be captured
- Measurement and acquisition system with 2 fast stereographic camera sets for net flight measurement and 3-axis accelerometer and gyroscope for microgravity conditions measurement (as plane is rotating during parabola, the net will experience some vertical drift as its flight direction is perpendicular to plane rotation axis)

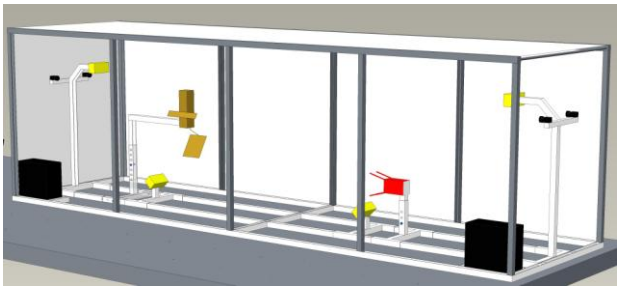

Fig. 9 Design of testing rig for parabolic flight model validation

Whole the rig is presented in Fig. 9. It will be covered with textile panels to provide proper background for cameras as well as for safety reasons.

For each of the experimental cases trajectories of all the knots within the net will be measured (see section 5) and results will compared to simulations of the same cases. Simulations will take into account real gravity indications from measurements, Coriolis drift of the net (due to rotational movement of the plane during parabola) and air drag (early calculations indicate that air drag will have relatively small but still significant influence on net trajectory).

Mathematical formalism of the validation is built upon weighted sum of squared distances between simulated and measured trajectories of all the knots in the net.

4.2 Material characterization

One of most important issues for experimental validation is characterization of material net is made of, so respective material properties may be used in reference simulations. 7 parameters are used in the model to describe the thread. They are summarized in following list with measurement methods used:

- Linear density - precise scales is used
- Stretching stiffness and damping - standard tensile machine is used. Stiffness is linearized around low forces, damping is estimated from stretching hysteresis.
- Bending stiffness and damping - cantilever method [11] is used for stiffness. It is extended with camera based measurement of damped oscillations.
- Torsional stiffness and damping - camera based measurement of torsional damped oscillations and fitting to damped harmonic oscillator model.

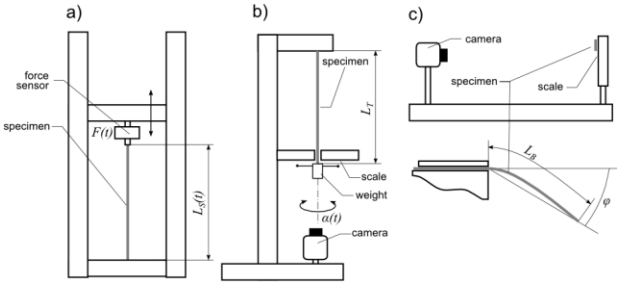

Fig. 10 Measurement schemes for yarn properties of stretching (a), torsion (b) and bending (c)

5 Measurement and Reconstruction

5.1 Cameras configuration

The experiment requires acquisition of color images with large resolution and relatively high depth of field.

The camera to be used in the experiment is VIEWROKS VC-4MC-C180EO-C**.** It has been chosen to minimize the acquired data size. It uses a single CMOS with Bayer filter instead of 3 CMOS (each for one main color – R, G, B) while preserving high image resolution. It is important to mind that a practical resolution is half the size of the catalogue one, for it will be used to acquire color images.

Fig. 9 and Fig. 11 presents the simplified sketch of test rig designed for the experiment. It consists of two pairs of cameras (one pair can be considered as a stereo camera set), four light sources, satellite model (debris) and a net ejector.

Stereo cameras are to be aligned in flight axis and facing each other. The appropriate distance between cameras is to be determined by taking into account the blind area (increasing with base distance) and distance accuracy (increasing with base distance). It is estimated that position: about 0.5 m above flight axis, about 1 m of base distance and no more than 7 m between stereo camera sets should meet the criteria.

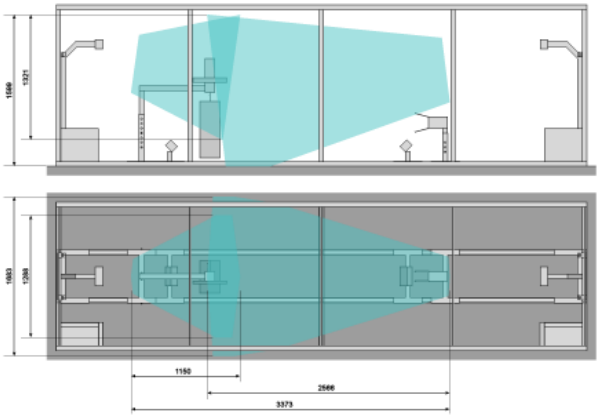

Fig. 11 Stereograpgic cameras working area

One set of cameras will be equipped with 16 mm lens, the other set with 25 mm. The expected working area of cameras is shown in Fig. 11.

To ensure the quality of moving object's picture the shutter time must be minimized and all 4 cameras are to be synchronized by global trigger. According to requirements regarding sampling frequency maximum speed of chosen cameras is 179 fps. It is also conditioned by expected maximum objects speed estimated at around 2.5 m/s.

The experiment conditions imply use of strong light source. It will be provided by 4 lamps (indicated in Fig. 9 with yellow boxes). The light can be provided by a halogen reflector of 500-1000W each, a fluorescent lamp reflector of 40kHz and 100W each or a LED reflector of 15-30W each. The set of lights and their arrangement will be tested and optimized on the rig. It will also affect the choice of aperture settings. The final values will be determined on the rig and result from compromise between the exposure time and iris size in the real light conditions.

Test rig will be constructed with black or white uniform walls providing best contrast with net's thread color. It is necessary as the mesh nodes will be identified by colors (see section 5.4).

5.2 Acquisition

The data will be collected during parabolic flights and stored for future analysis. Requirements for proper data acquisition system are calculated based on parabolic flight cycle and camera's parameters.

Having a camera of 2048×2048 pixels matrix, acquiring data at 179 fps we need to transfer data at about 750MB/s. This data is to be sent in real time to computer and subsequently to SSD disc by 263MB/s.

During whole parabolic flight one camera is estimated to generate about 300GB of data that will be stored on 500GB SSD disc. Not to operate at the limits of data throughput and for data safety acquisition will be performed by 4 independent computers – 1 per camera.

The data will be analyzed after acquisition in offline mode.

5.3 Environment identification

It is desirable for the cameras to work with same coordinates systems. It can be achieved in several ways. If possible it will be done with use of checker board or with help of the OptiTrace technology by OptiNav [12].

The first option is to calibrate the cameras before the experiment with use of checker foil placed in the working area common for both stereo cameras. The pattern is identical on both sides of the foil and visible for both camera's sets. Automatic alignment of cameras can be achieved by analyzing checker pattern on both images and aligning it. This operation simplifies following analysis.

Use of OptiTrace 3D markers is under consideration to improve performance and accurateness of the system. It will ensure linking of the cameras coordinate system with the one associated with plane. A set of markers will be evenly distributed in a pattern that is to be defined on the rig as well as on debris model and net ejector. This may be used to control the net's trajectory, indicate any unexpected disturbances during flight and to measure actual position and orientation of target and ejector. This is also a faster way to correct cameras position in case of undesired displacements that may occur since the experiment is to be run in dynamic conditions.

5.4 Knots identification

The net shall be represented as a set of knots that need to be unambiguously identified for tracking purpose. The reconstruction of the individual yarns is not necessary but it will be done if possible.

Each knot will be identified by a set of colors of its adjacent yarns. Several algorithms of net coloring have been taken into account from which one has been chosen as the most promising. Analysis of complexity and color palette size were used as differentiating factors between proposed solutions.

The chosen algorithm assigns one color for each yarn. One knot is then identified with a set of 2, 3 or 4 colors assigned to its neighboring yarns (yarns that directly goes to/from the node). The goal is to minimize the amount of colors used while preserving unambiguous marking of nodes.

The final algorithm will be optimized for the data collected during the parabolic flights, so it's final performance can be discussed afterwards.

5.5 Net reconstruction

The net 3D trajectory reconstruction is reduced to the problem of marking all 2D knots positions and label them with grid coordinates on each frame of the experiment record. However, simple manual labeling is not under consideration, as the number of nodes to be marked grows fast with size of net and time of experiment. Full automation of the process may be difficult to implement, especially on more complicated net configurations (post-launch, wrapping around debris). It is also associated with risk of mislabeling, what should be avoided at any cost. This is why automatic support for manual labeling seems to be the most promising solution.

The goal is to provide multiple tools to facilitate and speed up manual node labeling. Some examples of tools that can be provided are:

- Finding node inside circular area
- Finding path between two labeled nodes
- Filling grid in between closed path

The anticipated behavior of software is presented in Fig. 12.

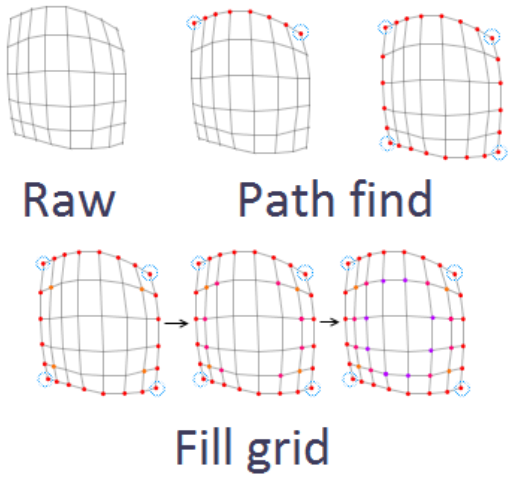

Fig. 12 Example procedure of semi-automatic node finding

With “Find Node” tool user will use circular cursor (similar to brush in graphics editors) to indicate the area in which automatic algorithm will search for intersection point. “Find Path” tool will allow to mark a whole row or column with fewer user actions. The algorithm will mark all intersection points on the shortest path between two nodes. “Fill Grid” tool will search for node in an area restricted to intersection of 3 spheres of radius equal to link length and center in already labeled neighbor knots. Starting from a set of labeled external knots it will be able to iteratively label remaining, internal knots.

The process of labeling nodes on sequential frames will be further supported by image processing techniques (motion tracking, optical flow).

The choice of algorithms, their performance and usefulness is to be verified after initial set of data is collected.

6 Conclusions

An approach of utilizing Cosserat rods model for simulation of net structures intended for space debris capturing has proven to be promising. It provides comparable results of related experiments as FEM simulations and it is also in good agreement with early physical experiments. As a model Cosserat rods seem to be particularly well suited to the application of capturing with nets as it reproduces most important aspects of yarn-like structures behavior – stretching, bending and torsion – still being efficient in implementation.

At time of this paper writing presented model is at early phase of implementation. Any significant optimization nor parallelization of code has not yet been performed, although by the nature of underlying mathematical model parallelization potential is very large. Therefore no performance benchmarks were performed, however even at this stage it is significantly faster than FEM simulations and real-time interactions are already possible. Also an appropriate contact algorithm is not yet implemented.

Full physical validation experiments are being designed. These experiments will be performed in parabolic flight and their role is not only to validate the model in its primary application – capturing of complex, inoperative target – but also to demonstrate and analyze whole the concept of net-like structure utilization for this purpose. Parabolic flight campaign is planned for autumn 2014.

Requirements for validation measurements are particularly demanding: relatively high velocities of net require high speed cameras and short shutter times. Thin threads net is composed of require high resolution. It leads to the complex acquisition system and demanding lighting conditions. Because of complex movement of the net during wrapping phase, postprocessing and full 3D reconstruction of individual knots trajectories can’t be fully automated. Instead semi-automated approach is proposed with unique color code for knots identification, special markers for environment recognition and supporting image analysis tools. Even with such tools reconstruction of trajectories from all experimental cases will be time consuming.

References

[1] J.-C Liou, N.L.Johnson, “Risks in space from orbiting debris”, Science, 311(5759): 340–341, January 2006.

[2] B. Bastida, H. Krag, “Analyzing the criteria for a stable environment”, AAS/AIAA Astrodynamics Specialist Conference, Girdwood, Alaska, 2011.

[3] “Robotic Geostationary Orbit Restorer. GSP phaseA final report”, Astrium SI, Bremen, June 2003. Doc no: ROG-SIBRE-FP.

[4] K.Wormnes, et.al, “ESA technologies for space debris remediation”, In 6th European Conference on Space Debris, Darmstadt, 2013.

[5] K.Wormnes et.al., “Throw-nets and tethers for robust space debris capture”, In IAC2013, Beijing, October 2013

[6] S.S. Antman, “Nonlinear problems of elasticity”, Springer-Verlag, 1995.

[7] J. Gratus, R.W. Tucker, “The dynamics of Cosserat nets”, Journal of Applied Mathematics 2003.4 (2003): pp. 187-226.

[8] D. Pai, “Strands: Interactive Simulation of Thin Solids Using Cosserat Models”, Computer Graphics Forum (Eurographics ’02), vol. 21, no. 3, pp. 347-352, 2002.

[9] J. Spillmann, M. Teschner, “CoRdE: Cosserat rod elements for the dynamic simulation of one-dimensional elastic objects”, Proceedings of the 2007 ACM SIGGRAPH/Eurographics symposium on Computer animation. Eurographics Association, 2007.

[10] H. Lang, J. Linn, M. Arnold, “Multibody dynamics simulation of geometrically exact Cosserat rods”, Berichte des Fraunhofer ITWM, Nr. 209 (2011)

[11] P. Szablewski, W. Kobza, “Numerical Analysis of Peirce’s Cantilever Test for the Bending Rigidity of Textiles”, Fibres & Textiles in Eastern Europe, 2003, Nr 4 (43), pp. 54-57

[12] http://optinav.pl/en/info/products/optiruler.html